Histidine Photodegradation during UV Resonance Raman Spectroscopy†

Qiang Wu, Gurusamy Balakrishnan, Alex Pevsner, and Thomas G. Spiro*

Department of Chemistry, Princeton University, Princeton, New Jersey 08544

Received: October 11, 2002; In Final Form: February 20, 2003

We report photodegradation of imidazole [ImH], 4-methylimidazole [4MeImH], and histidine during collection of UV resonance Raman [UVRR] spectra. The degradation rate of histidine residues in two proteins, Cu,Zn-superoxide dismutase (Cu,Zn-SOD) and the CO adduct of hemoglobin, was also examined. A two-photon mechanism is proposed for ImH, in which photoexcitation from an initially excited state produces $ImH^{\bullet+}$ cation radical, which deprotonates and dimerizes or reacts with other ImH molecules or with O_2. Photodegradation rates were measured for spherical and cylindrical focusing lenses, as well as for continuous wave and pulsed laser excitation. The cylindrical lenses slowed photodegradation 5-fold, while pulsed excitation (0.3 μJ, ∼20 ns, 1 kHz) speeded it up ∼2.5-fold. Histidine photodegradation is an insidious problem in protein UVRR spectroscopy because of the weakness of the histidine Raman signals. By keeping the laser power low and using cylindrical lenses, one can minimize damage to histidine while maintaining acceptable signal levels.

Introduction

There is increasing interest in applying ultraviolet resonance Raman [UVRR] spectroscopy to proteins.[1−5] The technique is a rich source of structural information because of resonance enhancement of Raman signals associated with UV chromophores, including aromatic residue side chains and the peptide bond itself. Histidine is a particularly important protein residue because its imidazole side chain is frequently involved in catalysis and in ligation of essential metal ions. Unfortunately, resonance enhancement of imidazole vibrations is weak,[6] and histidine UVRR bands are usually obscured by stronger signals from the rest of the protein. However, it has been possible to detect certain histidine signals when the imidazole is protonated[7] or bound to metal ions,[8,9] if the exchangeable protons are replaced by deuterium.

In the course of studying histidine UVRR spectra, we discovered novel signals, which led us to investigate the UV photochemistry of imidazole (ImH). Although there have been many previous studies of ImH and histidine photoreactions, they have been carried out with the aid of photosensitizers[10−13] and pulse radiolysis.[14] There seems not to have been previous detection of photoproducts from direct UV irradiation of ImH or histidine. We find direct photochemistry to be facile and, therefore, a challenge to the UVRR study of proteins. Precisely because histidine UVRR signals are weak, photodegradation of histidine residues is likely to go undetected in protein UVRR spectra. Fortunately, the photochemistry is multiphotonic, and it is possible to minimize this effect without losing the Raman spectrum by lowering the photon flux at the sample. To reduce the flux, we recommend the use of cylindrical focusing lenses instead of the more commonly used spherical lens. We report quantitation of these effects, as well as experimental results that characterize the nature of the photochemistry.

Materials and Methods

Sample Preparation. Imidazole, 4-methylimidazole, and histidine (Aldrich) were dissolved in 50 mM sodium phosphate buffer, which contained 0.1 M Na_2SO_4 as a Raman internal intensity standard. Aliquots either were deaerated with argon or remained aerated prior to laser irradiation; the deaerated samples were purged with nitrogen through a stir wire during irradiation. Bovine Cu,Zn-superoxide dismutase [SOD] was purchased from Sigma and used without further purification. Hemoglobin [Hb] was isolated from fresh human blood by standard procedures.[15] SOD (0.24 mM) and the CO adduct of hemoglobin A (HbCO, 0.17 mM) were exchanged into D_2O buffer (pD 7.4 sodium phosphate buffer, 50−100 mM) and purged with N_2 and CO, respectively, during the UV irradiation, as well as Raman measurements. The protein solutions contained 0.2 M $NaClO_4$ as the internal intensity standard.

Spectroscopy. An intracavity frequency-doubled CW argon laser (Coherent, FreD, 229 nm) was used for both irradiation and Raman excitation. The fouth harmonic of a Ti:sapphire laser (1 kHz, pulse width 20 ns) that was pumped by Q-switched Nd:YLF laser (Photonics International Inc., GM 30-527) was tuned to wavelengths 229, 218, and 206 nm. UVRR spectra were acquired with a Spex 1269 single monochromator equipped with an intensified photodiode array detector (Princeton Instruments). The 0.3 mL samples were contained in a Suprasil quartz NMR tube, which was spun around a stationary helical stirring wire for thorough mixing of the sample.[16] The laser power at the surface of the sample tube was kept at ∼0.3 mW. When a spherical lens ($f = 100$ mm) was used for focusing the beam, the estimated diffraction-limited diameter was ∼40 μm, giving a laser flux of 3.4×10^{19} photons cm^{-2} s^{-1}. Substitution of a combination of two cylindrical lenses ($f_1 = 200$ mm, $f_2 = 150$ mm) produced a 70×50 μm^2 rectangular focus and reduced the photon flux to 0.9×10^{19} photons cm^{-2} s^{-1}.

Each Raman spectrum was summed over 10 exposures of 60 s each. Spectra of acetone and cyclohexane, obtained under identical conditions, were used for frequency calibration. Raman intensities were measured relative to an internal standard,[17] the 981 cm^{-1} band of sulfate for ImH, 4-MeImH, and histidine, and the 933 cm^{-1} band of perchlorate for SOD and HbCO.

† Part of the special issue "A. C. Albrecht Memorial Issue".

10.1021/jp027190f CCC: $25.00
Published on Web 03/29/2003

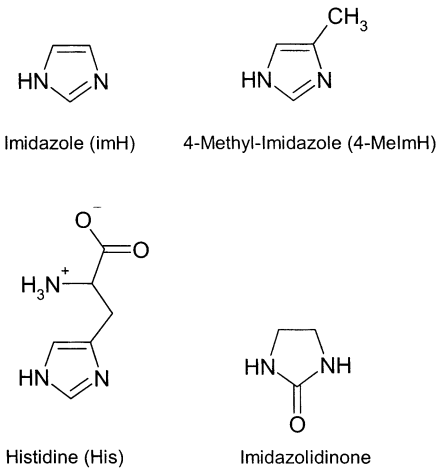

Figure 1. Structural diagrams of imidazole [ImH], 4-methylimidazole [4MeImH], histidine [His], and imidazolidinone.

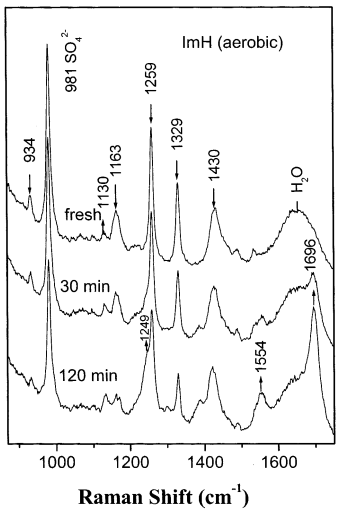

Figure 2. UVRR spectra of ImH (5.0 mM in pH 8.2 buffer containing 0.1 M Na_2SO_4) excited at 229 nm. The spectra were accumulated for 10 min at the indicated UV irradiation times (0.3 mW at the sample). Imidazole bands (↓) gradually disappear and are replaced by new bands (↑) from a photoproduct.

Absorption spectra were obtained with a HP8452 spectrophotometer.

Results

UVRR Spectra Reveal Imidazole Photodegradation. When aqueous ImH (Figure 1) is irradiated continuously with a 229 nm Raman laser, the Raman spectra gradually alter (Figure 2). The ImH peaks diminish over time, and a new set of bands at 1696, 1554, 1249, and 1130 cm^{-1} grow in. The new 1696 cm^{-1} band is at a higher frequency than any ImH mode. This band is most likely a carbonyl stretching vibration of one of the possible photoproducts. Probably it belongs to an imidazolidinone (Figure 1), as indicated by previous work on photosensitized oxidation of ImH.[18]

Deaeration of the sample slows the growth of photoproduct peaks (Figure 3), but the decay rate of ImH bands remains the same (Figure 4a), indicating that the primary photochemistry does not involve oxygen. Semilog plots of the ImH (1329 cm^{-1}) band intensity, relative to the internal standard (SO_4^{2-}, 981 cm^{-1}), show first-order behavior suggesting a single rate-limiting step. Similar behavior was observed for 4-methylimidazole (4-MeImH, Figure 1), a model compound for histidine. Again the decay rate was independent of aeration (Figure 4a).

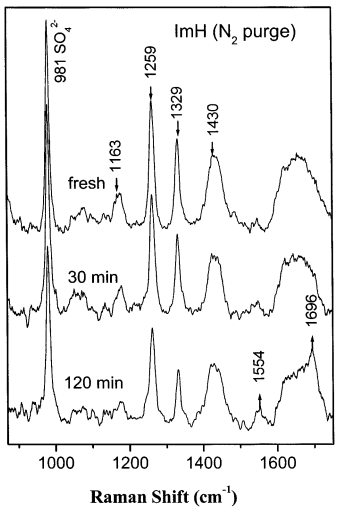

Figure 3. UVRR spectra of ImH (5.0 mM in pH 8.2 buffer containing 0.1 M Na_2SO_4) excited at 229 nm with N_2 purge. The spectra were accumulated for 10 min at the indicated UV irradiation times (0.3 mW at the sample). Imidazole bands (↓) gradually disappear but the growth of photoproduct bands (↑) is delayed.

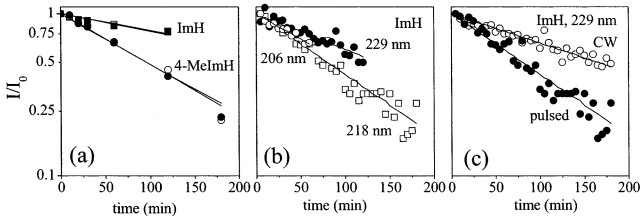

Figure 4. Semilog decay plots (a) for imidazole (1329 cm^{-1} UVRR band peak height, relative to SO_4^{2-}) and 4-methylimidazole (1230 cm^{-1}) with (□, ImH; ○, MeImH) and without (■, ImH; ●, MeImH) N_2 purge (conditions as in Figures 2 and 3 for both species), and for the 1329 cm^{-1} imidazole UVRR band (b) at three different pulsed (0.3 μJ, ~20 ns, 1 kHz) laser wavelengths and (c) under CW and pulsed irradiation, both at 0.3 mW average power.

TABLE 1: Photodegradation Rate Constants of Imidazole, 4-Methylimidazole, Histidine, and SOD under Continuous Wave (229 nm) Laser Irradiation with a Spherical Focusing Lens

		decay rate constants (10^{-4}/sec)	
species	pH/**pD**	aerobic	N_2 purge
ImH	8.2	2.2	2.4
4MeImH	8.2	3.1	3.0
His	8.2	2.9	1.6
	10.0		2.8
	7.4		1.9
	10.0		3.0
SOD	**7.4**		2.9

We also examined the photodegradation of ImH at 229, 218, and 206 nm using pulsed laser excitation from a frequency-quadrupled Ti:sapphire laser.[19] The shorter excitation wavelengths are of interest because they are better suited to protein secondary structural studies.[20,21] Although the absorptivity is much higher at 218 and 206 nm than at 229 nm, the decay rates are nearly the same (Figure 4b and Table 2). The density of photoexcited molecule is apparently compensated by the shorter laser path when the focus is adjusted in the absorbing sample (backscattering geometry). At 229 nm, the decay rate is ~2.5-fold higher for pulsed than for CW excitation (Figure 4c, Table 2) at the same average power (0.3 mW). This increase is consistent with the decay mechanism being multiphotonic (see below). However, the increase is smaller than might have been

TABLE 2: Photodegradation Rate Constants of Imidazole, SOD, and HbCO under Pulsed Laser Irradiation with Cylindrical Focusing Lenses

species	wavelengths (nm)	pH/**pD**	decay rate constants (10^{-4}/sec)[a]
ImH	229	8.2	1.6 (0.6)[b]
	218	8.2	1.8[b]
	206	8.2	1.2[b]
SOD	229	**7.4**	(0.6)[b]
HbCO	229	**7.4**	(0.6)[c]

[a] Values given in parentheses correspond to CW excitation. [b] Aerobic conditions. [c] Under CO.

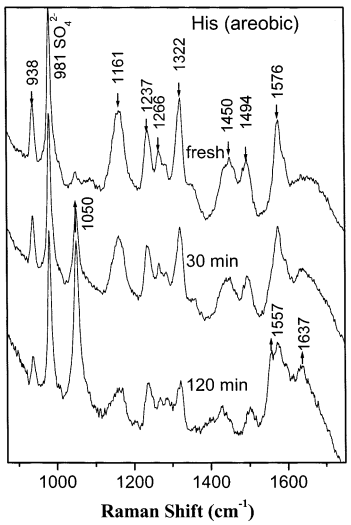

Figure 5. UVRR spectra of histidine (5.0 mM in pH 8.2 buffer containing 0.1 M Na_2SO_4) excited at 229 nm. The spectra were accumulated for 10 min at the indicated UV irradiation times (0.3 mW at the sample). Imidazole bands (↓) gradually disappear and are replaced by new bands (↑) from a photoproduct.

expected because the peak power of the 0.3 μJ, ~20 ns laser pulses, 15 W, is 50 times the average power. As discussed below, the photodegradation is complex.

Histidine Decay is Dependent on Aeration and on pH. Aqueous histidine (His, Figure 1) behaves similarly (Figure 5), although the photoproduct UVRR peaks at 1050, 1557, and 1637 cm^{-1} differ from those of ImH. Again the photoproduct peaks are suppressed by deaeration, and in this case, the decay of the histidine peaks is slowed in the absence of air in contrast to ImH. Moreover, the time course is multiexponential, indicating more than one reaction path. The initial slope in the absence of air gives a rate constant between those of ImH and 4-MeImH (Table 1). This rate increases by 75% at pH 10 (Table 1), suggesting involvement of deprotonation in the decay. Lowering the pH to 3 (D_2O) completely prevents the decay, indicating that protonation protects histidine from the photoreaction.

Histidine in Proteins. To investigate photodegradation of histidine residues in proteins, we examined Cu,Zn-SOD, for which several bands of metal-coordinated histidine have been identified in D_2O.[22] We chose the isolated 1050 cm^{-1} band of Zn-bound histidine to measure kinetics (Figure 6). The rate constant is close to the 4-MeImH rate constant (Table 1).

We also examined HbCO, which has 38 histidine residues. For this protein, the only quantifiable histidine UVRR signal is the 1407 cm^{-1} band of protonated histidine in D_2O.[7] To access the photodegradation rate at pD 7.4. we employed the following procedure. First, the intensity of 1407 cm^{-1} band was measured in a fresh solution at pD 5.0, in which most of the histidine

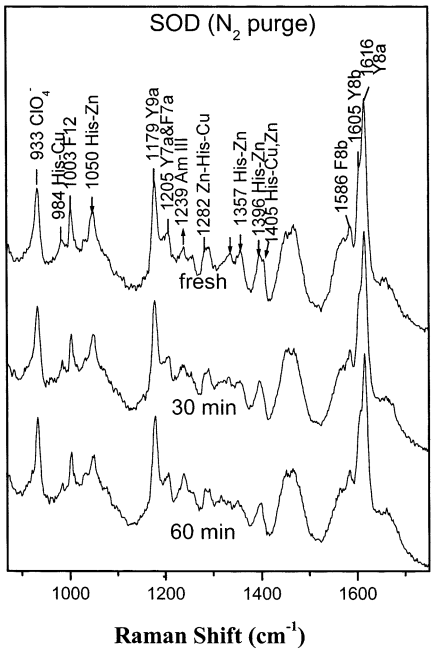

Figure 6. UVRR spectra of SOD (0.24 mM Cu,Zn-SOD, pD 7.4, 0.2 M $NaClO_4$) excited at 229 nm. The metal-bound histidine modes diminish with irradiation time. Assignments from ref 21.

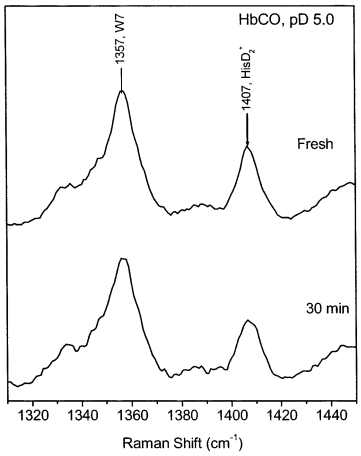

Figure 7. UVRR spectra of HbCO (0.17 mM in D_2O, pD 5.0, 0.2 M Na_2ClO_4) excited at 229 nm for fresh sample and sample after 30 min of laser irradiation at pD 7.4.

residues are protonated. Then the pD of the solution was increased to pD 7.4, and the sample was irradiated with the UV laser for 30 min. The pD of the irradiated sample was lowered to pD 5.0, and the intensity of 1407 cm^{-1} band was again measured (Figure 7). In this way, the loss of histidine at pD 7.4 could be monitored via the histidine-D^+ band. The decay rate in HbCO was essentially the same as that in SOD.

For both proteins, the decay of the histidine signals is significantly reduced by using a pair of cylindrical focusing lenses instead of the usual spherical lens. Cylindrical lenses reduce the photon flux at the sample by spreading the laser beam out into a line, instead of a spot, while improving the signal by matching the image shape with the entrance slit of the monochromator and the detector. The degradation rate constant for Cu,Zn-SOD was 5 times lower than that with the spherical focusing lens (Figure 8). With the cylindrical lenses, the decay of histidine bands in SOD or HbCO was only 4% during a 30 min spectral accumulation.

Absorption Spectra Reveal Multiple Products. To investigate the mechanism of imidazole degredation in the UVRR

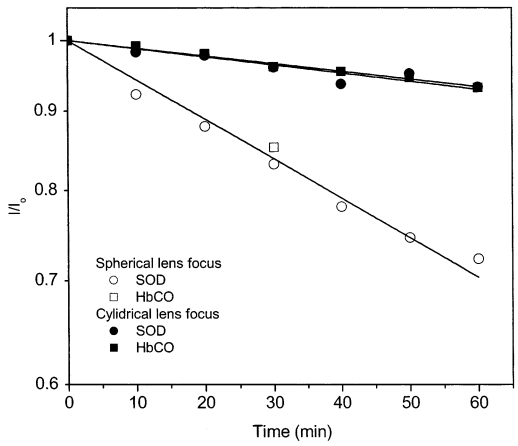

Figure 8. Semilog decay plots for histidine UVRR signals in Cu,Zn-SOD (0.24 mM, pD 7.4, 1050 cm^{-1} band, □) and HbCO (0.12 mM, pD 7.4, 1407 cm^{-1} band, ○). Empty and filled symbols are data obtained with spherical and cylindrical focusing lenses, respectively.

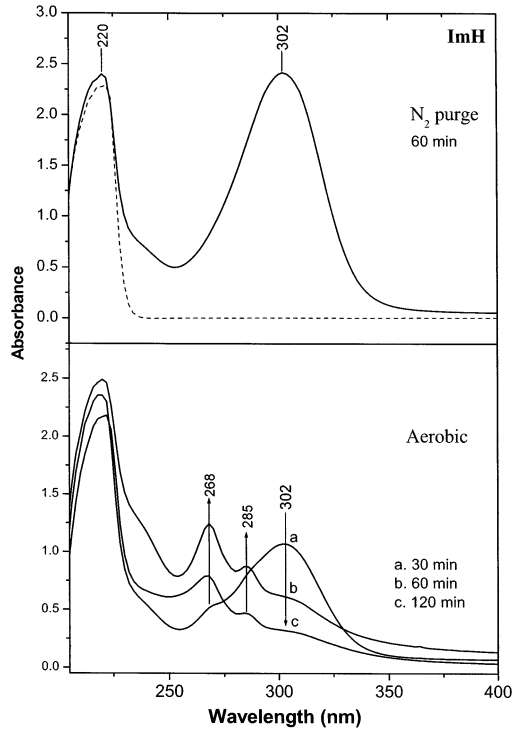

Figure 9. UV absorption spectra of ImH (A) fresh and after 60 min of 229 nm CW laser irradiation under a N_2 purge and, (B) at the indicated irradiation times in the presence of air. (5 mM, pH 8.2, 229 nm, 0.3 mW power, spherical focusing lens)

laser beam, we recorded UV absorption spectra under different conditions and discovered a number of photoproduct absorption bands at wavelengths below 350 nm [Figure 9]. When the sample is anaerobic, a 302 nm band rapidly grows in. After 60 min of irradiation, its intensity is comparable to that of the 220 nm absorption band of ImH itself. We have been unable to characterize the photoproduct using NMR or mass spectroscopy on irradiated solutions or their residues and conclude that the photoproduct is labile and formed in low yield. The 302 nm transition must be very strong.

When air is present during irradiation, the 302 nm photoproduct is gradually converted to other species, which absorb at 285, 268, and 230 nm. The 230 nm band is coincident with the 229 nm Raman laser wavelength and presumably gives rise to the aerobic photoproduct RR bands [Figure 2].

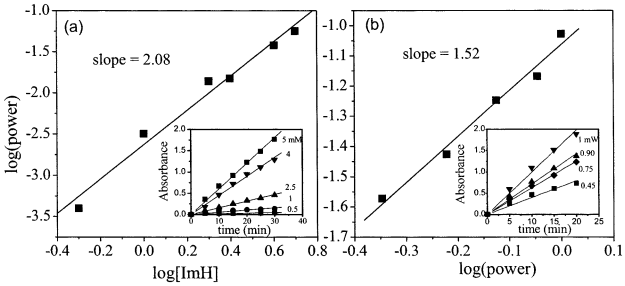

Figure 10. Log−log plot of the initial rate of 302 nm band formation vs (a) imidazole concentration and (b) laser power. The inset in panel a shows the time course at the indicated ImH concentration. Conditions: pH 8, N_2 purge, and 0.75 mW power at 229 nm using cylindrical focusing lenses. The inset in panel b shows the time course at the indicated laser power. Conditions: 5 mM ImH, pH 8 under N_2 purge using cylindrical focusing lenses.

To elucidate the nature of the photochemistry, we monitored the initial rate of formation of the 302 nm absorption band as a function of ImH concentration [Figure 10a]. A log−log plot yielded a straight line with a slope of 2.08, clearly establishing a second-order dependence and a bimolecular mechanism.

We also monitored the 302 nm absorption as a function of the laser power level [Figure 10b]. In this case, the log−log plot had a slope of 1.52, suggesting a combination of one- and two-photon processes.

Discussion

The photochemistry of imidazoles has been studied extensively with the aid of sensitizer dyes.[10−13] To our knowledge direct photochemistry using deep UV irradiation has not been investigated. Sensitized photochemistry involves formation of the sensitizer triplet state, which can then react with the target molecule via H atom abstraction or electron transfer, the products being then susceptible to attack by O_2 [type I photochemistry]. Alternatively, the sensitizer can convert triplet O_2 to singlet O_2, which then attacks the target molecule [type II photochemistry].

Irradiation with deep UV light can initiate type II photochemistry because O_2 absorbs at wavelengths below 240 nm and can be converted to the singlet state upon photoexcitation. It is likely that this mechanism accounts for histidine degrading faster in the presence of O_2 than in its absence [Figure 5] because singlet O_2 reacts especially rapidly with carboxylates.[23]

However, O_2 is not involved in the primary photochemistry of ImH, since the decay rate is the same whether O_2 is present or not [Table 1]. Direct photoexcitation of ImH is implicated. The 229 nm excitation wavelength is in the foot of the strong 220 nm absorption and can directly access the ImH excited state, albeit at low efficiency.

$$\mathrm{ImH} + h\nu \rightarrow \mathrm{ImH}^* \qquad (1)$$

The 220 nm band has been assigned to $\pi-\pi^*$ excitations,[6] but a $n-\pi^*$ transition occurs at slightly lower energy,[24] and the $n-\pi^*$ state is likely to be populated. Indirect evidence that the $n-\pi^*$ state is involved in the photochemistry comes from the observation that histidine photodegradation is not observed at pH 3 (data not shown). The $n-\pi^*$ energy is elevated by protonation of the imidazole N atom, whereas the $\pi-\pi^*$ state is not greatly affected.

Absorption of a second photon by the phooexcited ImH would lead to ionization, leaving an imidazole cation radical.

$$\mathrm{ImH}^* + h\nu \rightarrow \mathrm{ImH}^{\bullet+} + \mathrm{e}^- \qquad (2)$$

Involvement of a second photon is established by the laser power dependence of the formation rate of the 302 nm ImH photoproduct [Figure 10b] and by the dramatic reduction in histidine residue photodegradation when the irradiation is spread out with a cylindrical lens [Figure 8]. The fact that the laser power dependence gives a slope of 1.52 instead of 2.0 probably arises from photodecomposition of the 302 nm ImH photoproduct, which would reduce its rate of formation in direct proportion to the laser power.

The radical cation is expected to deprotonate:

$$ImH^{\bullet+} \rightarrow Im^{\bullet} + H^{+} \quad (3)$$

This explains the increase in histidine degradation rate at high pH [Table 1], if $Im^{\bullet}$ is the reactive species [singlet O_2 formation is also enhanced at high pH, but the pH dependence of histidine degradation was observed in the absence of O_2].

The faster degradation of 4-MeImH than of ImH [Figure 4a] is attributable to the electron-donating effect of the methyl substituent, which enhances the radical reactivity. The reaction of histidine, which also bears a methylene substituent on the imidazole ring, is also accelerated for the same reason, but not by as much as 4-MeImH, presumably because of the countervailing influence of the nearby amonium group. This countervailing influence is absent for histidine residues in the middle of proteins, where the amino acid is incorporated into the polypeptide chain. Interestingly, the decomposition of histidine residues in Cu,Zn-SOD is almost as fast as that of 4-MeImH, even though the imidazole rings are bound to metal ions.

Irradiation of ImH produces a 302 nm absorbing species. The second-order dependence on ImH concentration [Figure 10a] leads us to propose that this species is the radical dimer:

$$Im^{\bullet} + Im^{\bullet} \rightarrow Im{-}Im \quad (4)$$

The intense 302 nm absorption is then assigned to the $\sigma-\sigma^*$ transition of the weak interimidazole bond. This transition would be highly photoactive because the excited state is dissociative and reverses reaction 4. The 1.52 exponent in the laser power dependence can be explained on this basis.

When O_2 is present, it can rapidly react with $Im^{\bullet}$. Many products are likely, as has been observed in sensitized photochemistry.[25] The multiple UV absorptions that appear in the presence of O_2 [Figure 9] no doubt arise from those products that retain conjugation. One of these is imidazolidone [Figure 1], which is the likely source of the resonance-enhanced 1696 cm^{-1} photoproduct band [Figure 2] assignable to the C═O stretch. However, because the rate of ImH photodecomposition is independent of O_2, the main degradation pathway must involve $Im^{\bullet}$ attack on ImH itself. $H^{\bullet}$ atom abstraction, followed by rearrangement of the bonds, would destroy the conjugation, explaining the loss of resonance-enhanced UVRR signals.

In proteins, the photo-induced imidazole radicals are unlikely to dimerize and would instead react with protein side chains in their vicinity, or with O_2. However, radical generation would remain a two-photon process (although additional photoreactions may influence the laser power dependence of the decay rate).

Conclusions

The present observations have important implications for sample integrity in the UVRR spectroscopy of proteins. Histidine residues are demonstrably susceptible to photodegradation at quite modest laser power levels. Because UVRR scattering from imidazole is relatively weak, the histidine signals are overshadowed by those of the aromatic residues tryptophan, tyrosine, and phenylalanine. Consequently, histidine photodegradation is not easy to detect, yet the protein structure and function may be compromised. Deaeration does not afford protection because the primary photochemistry is independent of O_2.

Fortunately, the multiple-photon character of the photochemistry makes it possible to slow the process in a nonlinear fashion by lowering the laser photon flux. The collection of Raman spectra can be optimized with the use of cylindrical lenses to spread the irradiation into a rectangle, matching the spectrometer slit. In this way, it is possible to minimize histidine decomposition. The multiphoton photochemistry also makes pulsed laser excitation more damaging than CW excitation, but the increase in decay rate was found to be modest ($\sim 2.5\times$) for $\sim$20 ns, 1 kHz pulses.

Acknowledgment. This work was supported by NIH Grant GM 22578 from the National Institute of General Medical Sciences.

References and Notes

(1) Johnson, C. R.; Ludwig, M.; Asher, S. A. *J. Am. Chem. Soc.* **1986**, *108*, 905.
(2) Huang, S. C.; Peterson, E. S.; Ho, C.; Friedman, J. M. *Biochemistry* **1997**, *36*, 6197.
(3) Nagai, M.; Wajcman, H.; Lahary, A.; Nakatsukasa, T.; Nagatomo, S.; Kitagawa, T. *Biochemistry* **1999**, *38*, 1243.
(4) Hashimoto, S.; Takeuchi, H. *J. Am. Chem. Soc.* **1998**, *120*, 11012.
(5) Austin, J. C.; Jordan, T.; Spiro, T. G. In *Advances in Spectroscopy*; Clark, R. J. H., Hester, R. E., Eds.; John Wiley & Sons: New York, 1993; Vol. 20, pp. 55−127.
(6) Caswell, D. S.; Spiro, T. G. *J. Am. Chem. Soc.* **1986**, *108*, 6470.
(7) Zhao, X.; Wang, D.; Spiro, T. G. *J. Am. Chem. Soc.* **1998**, *120*, 8517.
(8) Zhao, X.; Wang, D.; Spiro, T. G. *Inorg. Chem.* **1998**, *37*, 5414.
(9) Vargek, M.; Zhao, X. J.; Lai, Z. H.; McLendon, G. L.; Spiro, T. G. *Inorg. Chem.* **1999**, *38*, 1372.
(10) Lukton, A.; Weisbrod, R.; Schlesinger, J. *Photochem. Photobiol.* **1965**, *4*, 277.
(11) Wolff, M. S. Imidazole Photooxidation. Ph.D. Dissertation, Yale University, New Haven, CT, 1970.
(12) Hasselmann, C.; Pigault, C.; Santus, R.; Laustriat, G. *Photochem. Photobiol.* **1978**, *27*, 13.
(13) George, M. V.; Bhat, V. *Chem. Rev.* **1979**, *79*, 447.
(14) Bansal, K. M.; Sellers, R. M. *J. Phys. Chem.* **1975**, *79*, 1775.
(15) Antonini, E; Brunori, M. *Hemoglobin and Myoglobin in their reactions with Ligands*; Elsvier: New York, 1971; pp 2−4.
(16) Rodgers, K. R.; Su, C.; Subramanian, S.; Spiro, T. G. *J. Am. Chem. Soc.* **1992**, *114*, 3697.
(17) Su, C.; Wang, Y.; Spiro, T. G. *J. Raman Spectrosc.* **1990**, *21*, 435.
(18) Wasserman, H. H.; Wolff, M. S.; Stiller, K.; Saito, I.; Pickett, J. E. *Tetrahedron* **1980**, *37*, 191.
(19) Zhao, X.; Chen, R.; Tengroth, C.; Spiro, T. G. *Appl. Spectrosc.* **1999**, *53*, 1200.
(20) Jordan, T.; Spiro, T. G. *J. Raman Spectrosc.* **1994**, *25*, 537.
(21) Asher, S, A.; Ianoul, A.; Mix, G.; Boyden, M. N.; Karnoup, A.; Diem, M.; Schweitzer-Stenner, R. *J. Am. Chem. Soc.* **2001**, *123*, 11775.
(22) Wang, D.; Zhao, X.; Vargek, M.; Spiro, T. G. *J. Am. Chem. Soc.* **2000**, *122*, 2193.
(23) Hartman, P. E.; Hartman, Z.; Ault, K. T. *Photochem. Photobiol.* **1990**, *51*, 59−66.
(24) Serrano-Andres, L.; Fulscher, M. P.; Roos, B. O. *J. Phys. Chem.* **1996**, *100*, 6484.
(25) Wasserman, H. H.; Stiller, K.; Floyd, M. B. *Tetrahedron. Lett.* **968**, *29*, 3277.